Toxicology in Vitro 29 (2015) 458–467

Contents lists available at ScienceDirect

Toxicology in Vitro

journal homepage: www.elsevier.com/locate/toxinvit

Nephroprotective effects of ferulic acid, Z-ligustilide and E-ligustilide isolated from *Angelica sinensis* against cisplatin toxicity *in vitro*

Valérian Bunel [a,b,*], Marie-Hélène Antoine [a], Joëlle Nortier [a], Pierre Duez [b,c], Caroline Stévigny [b]

[a] Laboratory of Experimental Nephrology, Faculty of Medicine, Université Libre de Bruxelles (ULB), Brussels, Belgium
[b] Laboratory of Pharmacognosy, Bromatology and Human Nutrition, Faculty of Pharmacy, Université Libre de Bruxelles (ULB), Brussels, Belgium
[c] Laboratory of Therapeutical Chemistry and Pharmacognosy, Université de Mons (UMONS), Mons, Belgium

ARTICLE INFO

Article history:
Received 22 August 2014
Accepted 24 December 2014
Available online 3 January 2015

Keywords:
Cisplatin
Ferulic acid
HK-2 cells
Ligustilide
Nephroprotection
Regeneration

ABSTRACT

Cisplatin (CisPt), a chemotherapeutic drug applied against solid tumors, is highly detrimental to the kidney. The risk of acute kidney injury implies adequate patient hydration to ensure sufficient diuresis; this strategy, now implemented in clinical practice, remains however incompletely satisfactory. New pharmacological approaches relying on the discovery of bioactive compounds need to be developed.

Based on previous studies reporting renoprotective activities for extracts of *Angelica sinensis* (Oliv.) Diels roots, three of its major active compounds, ferulic acid, Z-ligustilide and E-ligustilide, were investigated for possible alleviation of CisPt-induced nephrotoxicity. Five phenomena involved in acute kidney injury and subsequent fibrosis were investigated: *(i)* modulation of cell survival via reduction of the apoptosis rate; *(ii)* reduction of oxidative stress; *(iii)* improvement of tubular regeneration capacities through proliferation and migration; *(iv)* limitation of extracellular matrix and collagen deposition; and *(v)* prevention of the dedifferentiation processes via the β-catenin pathway.

Ferulic acid emerged as the most potent compound for alleviating cell death and collagen deposition, and for enhancing cell regeneration capacities. It also partially inhibited the β-catenin pathway, but was ineffective in lowering oxidative stress. Z- and E-ligustilides, however, were effective for limiting the oxidative stress, but only moderately affected other parameters. Ferulic acid appears to be a promising nephroprotective drug lead deserving further preclinical investigation.

1. Introduction

Cisplatin (CisPt) is an alkylating agent used in anticancer therapies for the treatment of a variety of solid-organ tumors. Although the drug is efficient in non-small cell lung carcinoma, testicular, ovarian, breast, head and neck cancers (Pabla and Dong, 2008), it is also detrimental to kidneys structure and function. This major drawback prohibits the use of higher doses and requires monitoring of the renal function during the treatment.

Similar to tumor cells, CisPt penetrates renal proximal tubular epithelial cells (RPTECs) in which it binds to DNA strands and proteins, inhibiting replication and translation, and thus cellular growth and proliferation (Jamieson and Lippard, 1999). Moreover, CisPt enhances the oxidative stress by the generation of reactive oxygen and nitrogen species (ROS/RNS) which are associated with damage to subcellular structures and macromolecules such as lipids, proteins or DNA (dos Santos et al., 2012). These two phenomena are the key elements that lead to DNA damage and eventually result in apoptotic or necrotic cell death pathways activation, processes responsible for the massive loss of RTECs along the nephron and, thus, for the loss of tubular function.

It is estimated that about 20–30% of patients treated with CisPt experience acute kidney injury (AKI) (Hilal et al., 2005; Yao et al., 2007). Until now, the only strategy able to limit nephrotoxicity, routinely applied in clinical practice, consists in a sufficient hydration of patients during treatment (Nortier and Sculier, 2011). However, the consequences of recurrent episodes of AKI – such as those experienced during CisPt treatment – are partially irreversible; and defects in tubular regeneration capacities can result in the onset

Abbreviations: AKI, acute kidney injury; ASAC, *Angelica sinensis* active compounds; CisPt, cisplatin; ECM, extracellular matrix; E-lig, E-ligustilide; FA, ferulic acid; ROS/RNS, reactive oxygen and nitrogen species; RPTEC, renal proximal tubular epithelial cell; Z-lig, Z-ligustilide.

* Corresponding author at: Laboratory of Experimental Nephrology, Campus Erasme, route de Lennik 808, 1070 Brussels, Belgium and Laboratory of Pharmacognosy, Bromatology and Human Nutrition, Bd du Triomphe, CP 205/9, 1050 Brussels, Belgium. Tel.: +32 25556184, +32 26505250; fax: +32 25556186, +32 26505430.

E-mail address: valerian.bunel@outlook.com (V. Bunel).

http://dx.doi.org/10.1016/j.tiv.2014.12.017
0887-2333/

and development of kidney fibrosis, a pathological condition associated with the definite loss of kidneys structure and function (Pabla and Dong, 2008).

In this context, there is a clear need to identify and validate new nephroprotective strategies, notably relying on pharmacological approaches (Barabas et al., 2008; dos Santos et al., 2012). These may be based on the study of herbal remedies issuing from Traditional Chinese Medicine (TCM) remedies. The roots of *Angelica sinensis* (Oliv.) Diels (Apiaceae), a TCM drug known as Danggui, have been traditionally used as a *blood tonic* to treat female sexual dysfunction such as menstrual disorders and menopausal symptoms (Chao and Lin, 2011; Low Dog, 2005). This herbal product is frequently associated with *Astragalus membranaceus* (Fisch.) Bge. for the treatment of kidney diseases in China; modern researches brought evidences of a renoprotective activity for both the combination or *A. sinensis* alone in clinical trials (Li and Wang, 2005), and in both *in vitro* (Bunel et al., 2014a; Meng et al., 2011; Wojcikowski et al., 2009) and *in vivo* (Cai et al., 2001; Meng et al., 2011; Song et al., 2009; Wang et al., 2004) studies.

In the present study, we assessed *in vitro* the nephroprotective potential of 3 molecules isolated from the roots of *A. sinensis*. The 2 major active compounds: ferulic acid (FA) and Z-ligustilide (Z-lig); and another less studied, but structurally close to Z-lig: E-ligustilide (E-lig) (Fig. 1) (*A. sinensis* active compounds, ASAC) (Chen et al., 2013). Five key phenomena involved in CisPt-induced AKI and responsible for the onset and development of kidney fibrosis were investigated: *(i)* cellular death mediated by apoptosis (Havasi and Borkan, 2011; Pabla and Dong, 2008; Wynn, 2010); *(ii)* increased generation of ROS/RNS; *(iii)* tubular regeneration capacities of healthy cells (Lee and Kalluri, 2010; Megyesi et al., 2002; Wynn, 2010); *(iv)* extracellular matrix (ECM) deposition, involving notably collagen (Wynn, 2010; Yang et al., 2010); and *(v)* dedifferentiation processes of epithelial cells via β-catenin relocalization (Hao et al., 2011; Liu, 2010).

2. Materials and methods

2.1. Cell culture and treatment

HK-2 cells, originating from RPTECs, were obtained from American Type Culture Collection (CRL-2190, ATCC, USA), and grown in low glucose DMEM containing 10% fetal bovine serum (FBS PAA Clone, PAA laboratories, Pasching, Austria), 2 mM L-glutamine and 1% penicillin–streptomycin. Cells were sub-cultured or harvested for experiments when reaching about 90% confluence. For experimental purposes, cells were used between passages 6 and 25, harvested by trypsinization and seeded on 6-well plates (3×10^5 cells), 12-well plates (1×10^5 cells), 8-well chambered slides (Lab-Tek II, Nunc, Rochester, USA) (8×10^4 cells) or 96-well plates (1×10^4 cells). Next, cells were incubated for 24 h in FBS-containing medium, rinsed twice with DMEM and treated with test substances in FBS-depleted medium.

CisPt solutions were prepared from the marketed drug Cisplatine Hospira® (Hospira Benelux, Antwerpen, Belgium) and cell treatments were performed with at 10 μM, a concentration close to its IC_{25} after 48 h incubation (Fig. 1S). FA (purity 99.3%) was purchased from Sigma–Aldrich (St. Louis, USA); E-lig (purity 99.1%) from Extrasynthèse (Genay, France); and Z-lig (purity 99.5%) from Sequoia Research Products (Pangbourne, United-Kingdom). Stock solution were prepared in DMSO and stored at −80 °C until use.

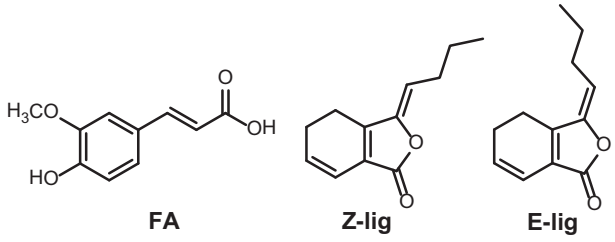

Fig. 1. Structure of the ASAC selected for this study: ferulic acid (FA), Z-ligustilide (Z-lig) and E-ligustilide (E-lig).

2.2. Cell viability assay

2.2.1. Resazurin assay

Cells were treated with CisPt and/or ASAC in 96-well plates, washed twice with PBS, and assessed for their viability by incubation with 0.44 mM resazurin solution (Sigma–Aldrich, St. Louis, USA) for 1.5 h at 37 °C. Absorbances were measured at wavelengths 540 and 620 nm using a iEMS Reader MF spectrophotometer (Thermo Labsystems, Breda, The Netherlands). Percentages of reduced dye were calculated with the following formula:

$$\frac{(\varepsilon OX)\lambda 2 \cdot A\lambda 1 - (\varepsilon OX)\lambda 1 \cdot A\lambda 2}{(\varepsilon RED)\lambda 1 \cdot A'\lambda 2 - \varepsilon RED)\lambda 2 \cdot A'\lambda 1}$$

where εOX = molar extinction coefficient of resazurin (47.6 at 540 nm and 34.8 at 620 nm); εRED = molar extinction coefficient of resorufin (104.4 at 540 nm and 5.5 at 620 nm); A = absorbance of test wells; A' = mean absorbance of blank wells; $\lambda 1$ = 540 nm; $\lambda 2$ = 620 nm. Viability (*i.e.* metabolic activity) was normalized against control condition.

2.2.2. Protein assessment

Cells were treated in 96-well plates, rinsed with PBS and lysed with Cell Lysis Bruffer (BD Pharmingen, San Diego, USA). Protein amounts were assessed with the Pierce BCA Protein Assay kit (Thermo Scientific, Rockford, USA) following the manufacturer's instructions. Absorbances were measured at wavelength 540 nm using a iEMS Reader MF spectrophotometer. Protein amounts were expressed as percentages of control condition.

2.2.3. Annexin V/propidium iodide staining assay

Cells were treated with ASAC and/or CisPt in 12-well plates, harvested and centrifuged at 1400×. Supernatants were discarded and cells were resuspended and incubated with Annexin V-FITC detection kit (BD Pharmingen, San Diego, USA) in the dark for 15 min. Suspensions were then analyzed using a BD FACSCanto II flow cytometer (BD Pharmingen, San Diego, USA) and 10^4 cells were recorded. The data were analyzed with FlowJo software (Tree Star, Ashland, USA); debris and cell clumps were removed by gating and the proportions of live, apoptotic and necrotic cells were calculated.

2.3. Evaluation of protective effect towards oxidative stress

2.3.1. DPPH assay

The antioxidant activities were assessed by measurement of the scavenging ability of ASAC towards the stable free radical 2,2′-diphenyl-1-picrylhydrazyl (DPPH). Serial dilutions of test compounds (FA, Z-lig, E-lig and Trolox® used as a reference) were made and a 0.004% DPPH methanolic solution was added to 96-well plates. Mixtures were left to react for 30 min in the dark; the absorbances were measured at wavelengths 540 and 620 nm with a iEMS Reader MF spectrophotometer. The results were fitted to the following parametric function:

$$N = N_0 \cdot e^{-kC}$$

where C = concentration; N = percentage of DPPH remaining at concentration C; N_0 = percentage of DPPH at concentration 0 and k = the parameter.

The IC_{50} was calculated for each compound and results were expressed as Trolox® equivalent antioxidant capacity (TEAC = IC_{50} Trolox®/IC_{50} compound).

2.3.2. H_2DCF-DA oxidation for ROS measurement

Cells were treated with ASAC and/or CisPt in 12-well plates, rinsed and treated with 10 μM 2′,7′-dichlorodihydrofluorescein diacetate (H_2DCF-DA) solution (Sigma–Aldrich, St. Louis, USA). Cells were harvested, centrifuged at 1400× and analyzed using a BD FACSCanto II flow cytometer. A total of 10^4 cells were recorded. The data were analyzed with FlowJo software; debris and cell clumps were removed by gating and mean fluorescence intensities (MFI; geometric mean) were estimated.

2.3.3. Ki-67 immunostaining

Cells were treated for 48 h on chambered slides, rinsed with PBS, fixed in 4% paraformaldehyde solution for 20 min, rinsed and permeabilized with 0.01% Triton X for 5 min. Cells were blocked with goat serum (PAA Laboratories, Austria) for 1 h and incubated with a primary rabbit anti-Ki-67 antibody (Abcam, Cambridge, UK) for 1 h. Slides were rinsed twice and incubated with a secondary Alexa Fluor 488 conjugated goat anti-rabbit antibody (Invitrogen, Eugene, USA) for 30 min. Slides were rinsed twice, mounted with DAPI-containing mountant (Invitrogen, Eugene, USA) and examined with an Axioskop fluorescence microscope (Zeiss, Germany) at magnification 400×. Twenty pictures per chamber were acquired. The Ki-67 index was calculated by dividing the number of Ki-67 positive cells by the total number of cells (Yang et al., 2010).

2.3.4. Cell cycle analysis

Following treatment in 12-well plates, cells were harvested and fixed with 66% ethanol for 1 h at 4 °C. Pellets were centrifuged at 1400× and rinsed with PBS, resuspended in PI/RNase Staining Buffer (BD Pharmingen, San Diego, USA) following the manufacturer's instructions and incubated 30 min at room temperature. Cells were washed, resuspended and analyzed using a BD FACSCanto II flow cytometer. A total of 10^4 HK-2 cells were recorded using the BP 585/42 filter at a maximum rate of 200 events/s.

Cell cycle analysis was achieved with FlowJo software: debris and cell clumps were removed by gating and proportions of G0/G1, S and G2/M cells were determined according to the Dean-Jett-Fox model (Anonymous, 2011).

2.3.5. Wound healing assay

Cells were seeded on 60-mm Petri dishes, incubated for 48 h, yielding approximately 90–100% confluence and were growth arrested by serum starvation for 24 h. Linear scratches were made through cell monolayers with a sterile 200 μl pipette tip. Debris were removed and 10 pictures were taken (time t_0) using a Motic AE21 microscope equipped with a Moticam 2300 camera (Motic, Wetzlar, Germany) at magnification 100×. Cells were then treated with test substances for 18 h, and 10 new pictures of the scratch were taken (time t_{18}).

The area of the scratch was measured using TScratch (Geback et al., 2009) and the migration rates (μm/h) were calculated.

2.3.6. Assessment of collagen synthesis

Cells were treated in 96-well plates, rinsed with PBS and assessed for their metabolic activity with the resazurin assay as described above. Then, cells were washed with PBS, fixed with ice-cold methanol for 1 h at 4 °C, rinsed twice with 1% acetic acid and stained for 2 h with 0.1% picrosirius red (PSR) staining solution (Hu et al., 2009). Wells were then rinsed three times with 1% acetic acid. The dye was solubilized in 0.1 M NaOH and absorbances of the wells were measured at wavelength 540 nm. Absorbances attributed to PSR staining were normalized according to the metabolic activity of each well (the correlation between the number of cells, metabolic activity and protein amount determined by the bicinchoninic acid method was verified in preliminary experiments (Supplementary data, Fig. 4S)).

2.4. β-Catenin determinations

2.4.1. Membranous β-catenin determination

The amounts of membranous β-catenin were evaluated with a quantitative fluorescence image analysis (QFIA) technique. Cells were treated on 8-well chambered slides, rinsed with PBS and fixed in 4% paraformaldehyde solution for 20 min. Slides were rinsed and permeabilized with 0.01% Triton X for 5 min. Slides were rinsed again and cells were blocked with donkey serum (sc-2044, Santa Cruz Biotechnology, Santa Cruz, USA) for 1 h. They were then incubated with mouse anti-human β-catenin primary antibody (sc-7963, Santa Cruz Biotechnology, Santa Cruz, USA) for 1 h, washed twice, incubated with cyanine-3 conjugated donkey anti-mouse secondary antibody (715-166-151, Immuno Research Lab Jackson) for 30 min, rinsed twice, mounted with DAPI-containing Prolong Gold antifade reagent (Invitrogen, Eugene, USA) and examined at magnification 400× with an Axioskop fluorescence microscope (Zeiss, Germany) equipped with a DP200 camera (Deltapix, Maalov, Denmark).

Prior to the evaluation of fluorescence intensity, the domain of linearity and the reproducibility of the method were checked using Inspeck™ Orange (λ_{Ex} = 540 nm/λ_{Em} = 560 nm) fluorescently labeled microbeads (6.0 μm diameter) (Molecular Probes, Eugene, USA).

For each condition, 10 pictures were taken, and analyzed using Fiji (Fiji Is Just ImageJ) software. The fluorescence intensity was evaluated by the measurement of luminance. The nuclei were counterstained with DAPI. The blue-fluorescent areas were discarded from the pictures, allowing removal of eventual signals corresponding to nuclear β-catenin.

2.4.2. Cytoplasmic/nuclear β-catenin determination

Cells were treated in 12-well plates, harvested, centrifuged at 500× and fixed in Cytofix/Cytoperm solution (BD Pharmingen, San Diego, USA) for 20 min at 4 °C. Suspension was washed twice, incubated with anti-human β-catenin-phycoerythrin monoclonal antibody (R&D Systems, Minneapolis, USA) in the dark for 30 min. Cells were washed twice and analyzed using a BD FACSCanto II flow cytometer. A minimum 10^4 cells were recorded. The data were analyzed with FlowJo software: debris and cell clumps were removed and mean fluorescence intensities (MFI; geometric mean) were calculated.

2.4.3. Statistical analysis

Unless stated otherwise, experiments were performed 4 times using independent samples. Results needing to be normalized vs. controls were treated as described previously (Valcu and Valcu, 2011). Data were compared by means of one-way ANOVA with post hoc Student's t test (Bonferroni correction) using GraphPad Prism 5 software and p values < 0.05 were considered significant.

3. Results

3.1. FA protects HK-2 cells against CisPt-induced mortality

After treatment with 10 μM CisPt for 24, 48 or 72 h, HK-2 cells survival dropped to 89 ± 2%, 74 ± 3% and 58 ± 3%, respectively, as compared to the control condition (Fig. 2). The 3 tested concentrations of FA, 50, 10 and 1 μM, could alleviate the CisPt-induced

mortality to respectively 98 ± 4%, 94 ± 3% and 92 ± 3% (n.s) at 24 h; to 84 ± 3%, 80 ± 3% and 78 ± 4% (n.s) at 48 h; and to 76 ± 5%, 67 ± 4% and 64 ± 3% at 72 h.

No statistically significant modifications were observed for co-treatment of cells with CisPt and Z-lig as compared to CisPt alone. Interestingly, 50 μM E-lig could decrease cell survival to 86 ± 2%, to 67 ± 5% and to 49 ± 4% for 24, 48 or 72 h incubation, respectively. In order to confirm if E-lig really enhanced the toxicity of CisPt, leading to an increased cellular mortality, the resazurin viability test was repeated in the absence of CisPt.

3.2. E-lig restrains metabolic activity and FA stimulates cellular proliferation

Fig. 2S (Supplementary data) suggests that treatment of cells with 50 μM E-lig alone decreased the metabolic activity (resazurin assay) to 87 ± 6% and 71 ± 8% after 48 and 72 h incubation, respectively, as compared to the control condition. However, the assessment of protein amounts carried out in the same conditions did not highlight any difference as compared to the control condition (Fig. 3S): this indicates that E-lig decreases the metabolic activity of HK-2 cells without inducing a loss of proteins, *i.e.* a loss of cells.

Moreover, FA tends to increase the metabolic activity as compared to control condition to 110 ± 2% and 106 ± 4% (n.s) after 48 h, and to 115 ± 7% and 111 ± 4% (n.s) after 72 h for concentrations of 50 and 10 μM, respectively (Fig. 2S). This increased metabolic activity was assorted with a higher protein synthesis to 112 ± 2% after 72 h (Fig. 3S), suggesting an improved cellular proliferation.

3.3. FA and Z-lig reduce CisPt-induced apoptosis

The beneficial effects of ASAC observed in cell survival were confirmed by investigating the apoptosis rates using a flow cytometric determination based on annexin V/PI staining. This technique allows differentiating viable cells from those undergoing necrosis or early and late phases of apoptosis. In our experimental setting, necrosis could not be observed as the triggering of this process is associated with higher doses of CisPt (dos Santos et al., 2012).

Treating the cells with 10 μM CisPt induced an increase in the amount of apoptotic cells to 3.1, 3.4 and 3.9-fold over the control condition after 24, 48 or 72 h, respectively (Fig. 3).

Upon co-treatment with FA, the enhanced apoptosis rates were limited to increases ranging between 1.2 and 2.2-fold over control condition, suggesting that FA could efficiently reduce cellular death as observed with the resazurin assay. Furthermore, FA had a dose–effect relationship on lowering CisPt-induced apoptosis at each of the investigated time-points. The highest dose of Z-lig also demonstrated an ability to reduce the apoptosis rate at the 3 tested time-points, whereas E-lig did not produce any significant effect as compared to CisPt treatment.

3.4. Effects of ASAC on oxidative stress

The effects of each compound on oxidative stress were evaluated by calculation of their TEAC which estimates their radical scavenging capacities. Ferulic acid being a potent antioxidant had a TEAC of 2.1. However, for both Z- and E-ligustilide, no TEAC could be calculated as there was practically no DDPH neutralization within the tested concentration range (Fig. 4A).

Surprisingly, only Z-lig and E-lig had an impact on ROS/RNS scavenging *in cellulo*: after 24 h treatment with CisPt, the generation of ROS raised to 151.5 ± 5.1% as compared to the control condition (Fig. 4B). Both Z-lig and E-lig (50 μM) could restrain oxidative stress to 100.8 ± 5.6% and 86.0 ± 10.4%, respectively. Lower doses of ligustilides did not produce any effect. Ferulic acid, at the 3 tested concentrations, could not reduce the oxidation of H_2DCF-DA probe.

3.5. Study of regeneration capacities modulation

3.5.1. Evaluation of cellular proliferation

In order to evaluate if ASAC can improve the proliferation of healthy RPTECs, HK-2 cells were treated for 48 h with test substances and stained for Ki-67 protein by immunofluorescence. FBS was used as a positive control; indeed, the proliferation of HK-2 cells has been shown to notably depend on EGF (epidermal growth factor) that is present in FBS (Ryan et al., 1994). FBS effectively induced a Ki-67 index increase of 326 ± 9% as compared to the serum-deprived control condition (Fig. 5A).

All the studied compounds increased the Ki-67 index: FA, Z-lig and E-lig demonstrated a dose–effect relationship. However, the largest magnitude across the 3 tested doses was observed for FA (ranging from 227 ± 13% to 194 ± 9% for 50 and 1 μM, respectively). (see Fig. 6).

CisPt treatment could also increase the proliferation index to 224 ± 10%. This has to be regarded as the consequence of its toxicity: in binding to nucleic acids and in generating higher amounts of ROS/RNS, CisPt causes damage to DNA that trigger a cell cycle

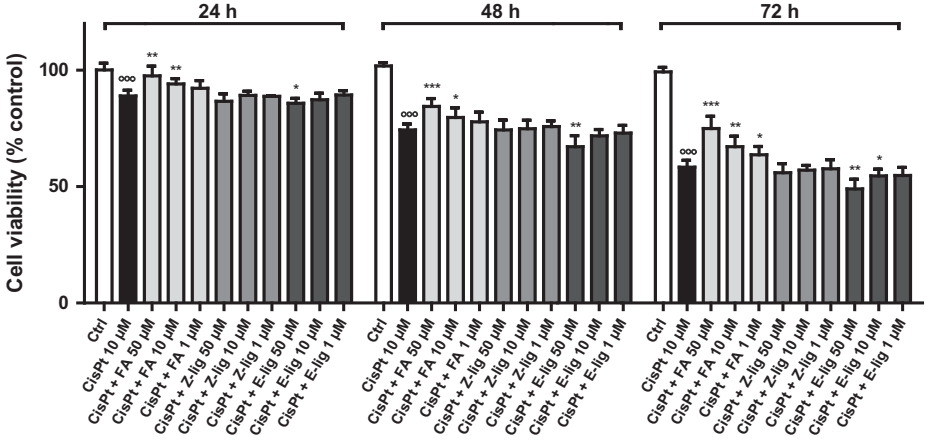

Fig. 2. Cell survival estimated with the resazurin assay. HK-2 cells were incubated for 24, 48 or 72 h with test compounds. Results are presented as means ± SD of 6 independent experiments performed in 6 replicates (°°°: $p < 0.001$ vs. Ctrl/*: $p < 0.05$; **: $p < 0.01$; ***: $p < 0.001$ vs. CisPt).

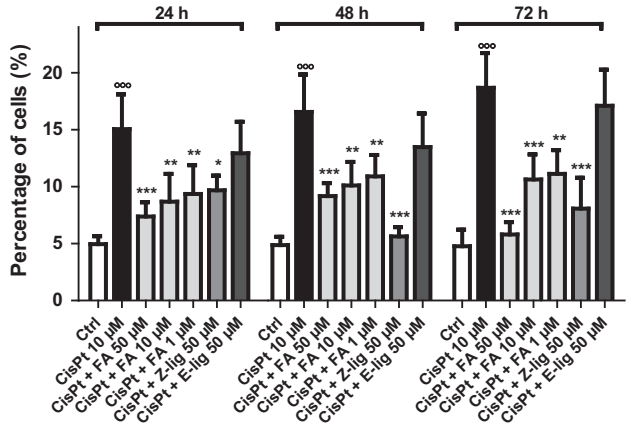

Fig. 3. Proportions of apoptotic cells after treatment with test compounds for 24, 48 or 72 h and determined by flow cytometry following Annexin V/PI staining. Results are displayed as means ± SD of 4 independent experiments (°°°: $p < 0.001$ vs. Ctrl/*: $p < 0.05$; **: $p < 0.01$; ***: $p < 0.001$ vs. CisPt).

arrest at the G2/M checkpoint, leading to an artificially higher Ki-67 index (Bunel et al., 2014b; Jamieson and Lippard, 1999) (see Fig. 5).

In order to verify if the increased Ki-67 index observed for ASAC is the consequence of a potential toxicity or is associated with a real enhancement in cellular proliferation, a cell cycle analysis has been performed.

FBS induced a slight decrease in the proportion of G0/G1 cells (76.0 ± 2.8% vs. 85.8 ± 2.4% for the control condition) and a slight increase in the proportion of G2/M cells (18.4 ± 2.7% vs. 8.8 ± 0.8% for the control condition). CisPt treatment triggered G2/M checkpoint arrest, resulting in a sharp decrease in G0/G1 cells (10.2 ± 0.8%) assorted with a sharp increase in G2/M cells (83.2 ± 3.9%).

Comparison of the profiles obtained for ASAC ruled out a G2/M increase similar to the one observed for CisPt, discarding a possible toxicity-induced Ki-67 increase.

Altogether, these results indicate that all the tested molecules could improve HK-2 cell proliferation.

3.5.2. Evaluation of cellular migration capacity

In order to evaluate the motility of cells, the scratch assay aimed at evaluating the migration rate of cells treated with test substances. FBS induced a 1.9-fold increase over the control condition (Fig. 6). Among the studied ASAC, only FA enhanced the cellular migration in a concentration dependent manner to about 1.7, 1.6 and 1.4-fold over the control condition, for doses of 50, 10 and 1 µM, respectively. Z-lig could not induce any statistically significant change. Finally, the highest dose of E-lig slowed down the migration of HK-cells to about 0.7-fold compared to control condition.

3.5.3. FA reduces collagen deposition

The production of ECM, investigated via the deposition of collagen and PSR staining, was assessed as previously described (Hu et al., 2009; Xu et al., 2007). In our experimental settings, CisPt induced a 135 ± 4% increase over control condition (Fig. 7). This increase could by limited by 50, 10 and 1 µM FA to augmentations of 112 ± 2%, 120 ± 3% and 126 ± 3%, respectively. Z-lig and E-lig did not induce any modification at the tested concentrations.

3.6. Evaluation of β-catenin relocalization

3.6.1. Membranous β-catenin

The amounts of membranous β-catenin were measured with a quantitative fluorescence image analysis (QFIA) method. HK-2 cells were treated for 48 h with test compounds and stained with specific immunofluorescence antibodies couple.

In the absence of CisPt, doses of 50 µM of each ASAC induced higher fluorescence signals for membranous β-catenin to about 1.2-fold over the control condition (Fig. 8A). At the exception of 10 µM FA, other doses of ASAC did not increase fluorescence. This indicates that FA is the most effective compound for the promotion of membranous β-catenin acquisition (hence the epithelial phenotype) under normal conditions.

When cells were treated with 10 µM CisPt, membranous β-catenin amounts dropped to about 50% compared to control. This decrease could be limited by the addition of 50 µM of FA, Z-lig and E-lig to about 80%, 80% and 70%, respectively. At 10 µM, FA was also effective in limiting this decrease to 70%, whereas other treatments did not produce any statistically significant difference. Once again, FA had the most promising activity in preventing the cells from losing membranous β-catenin following CisPt treatment.

3.6.2. Intracytoplasmic/nuclear β-catenin

Upon treatment of HK-2 cells with 10 µM CisPt, immunostaining and flow cytometry analysis of the intracytoplasmic/nuclear

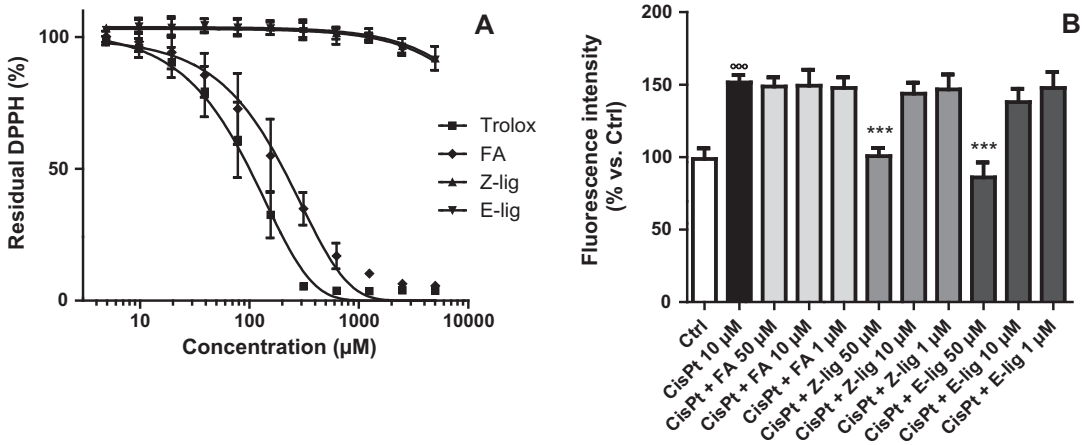

Fig. 4. DPPH neutralization curves obtained for ASAC (3 independent experiments performed in 8 replicates) **(A)**. The radical scavenging capacity, expressed as a Trolox equivalent (TEAC) was calculated by means of IC_{50} extrapolated from the curves. Fluorescence intensities recorded after flow cytometry assessment of HK-2 cells incubated for 24 h with ASAC and probed with 10 µM H_2DCF-DA **(B)**. Results are displayed as means ± SD of 4 independent experiments (°°°: $p < 0.001$ vs. Ctrl/***: $p < 0.001$ vs. CisPt).

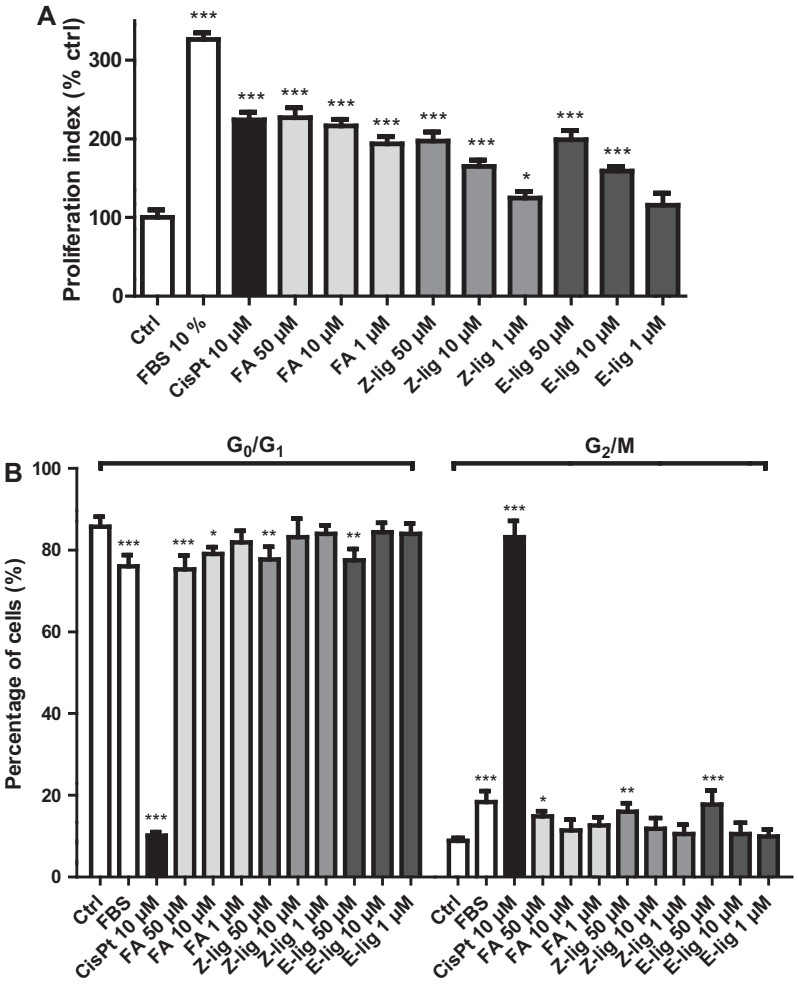

Fig. 5. Ki-67 evaluation of cells treated for 48 h with test substances **(A)**. Cell cycle phases (G_0/G_1 or G_2/M) distribution of cells treated in the same condition (proportions of cells in S-phases range from 4.8% to 9.8%; these are not statistically different between experiments) **(B)**. Results are displayed as means ± SD of 4 independent experiments (*: $p < 0.05$; **: $p < 0.01$; ***: $p < 0.001$ vs. Ctrl).

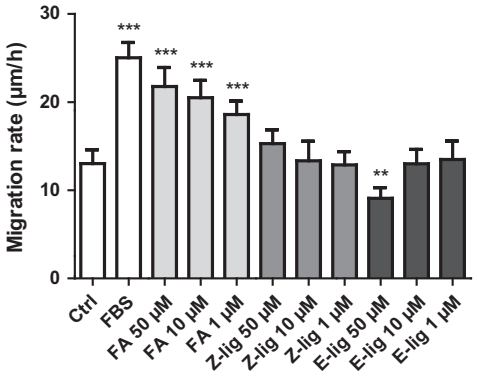

Fig. 6. Migration rates determined by the scratch assay for HK-2 cells after 24 h serum-deprivation. Monolayers were scratched with a pipette tip and incubated with test substances for 18 h. Migration rates are displayed as means ± SD of 6 independent experiments (**: $p < 0.01$; ***: $p < 0.001$ as compared to control conditions).

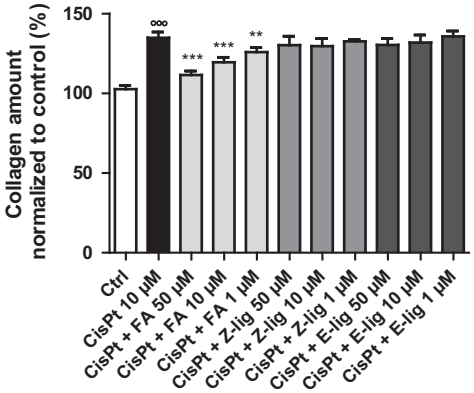

Fig. 7. Collagen quantification upon treatment of HK-2 cells with test substances for 48 h and PSR staining. Absorbances were normalized according to the metabolic activity (resazurin assay) and compared to the control condition. Results are displayed as means ± SD of 4 independent experiments performed in 6 replicates (°°°: $p < 0.001$ vs. Ctrl/**: $p < 0.01$; ***: $p < 0.001$ vs. CisPt).

β-catenin revealed a 2.5-fold increase over the control condition in the relocalizing form of the protein (Fig. 8B). All the ASAC, at every tested concentration, had similar efficacy in lowering this augmentation to about 1.7–1.9-fold over the control.

Altogether, these results indicate that FA is the most potent drug for *(i)* improving the acquisition of membranous β-catenin, and hence the epithelial phenotype of HK-2 cells; and *(ii)* avoiding the relocalization of β-catenin from membrane to the nucleus.

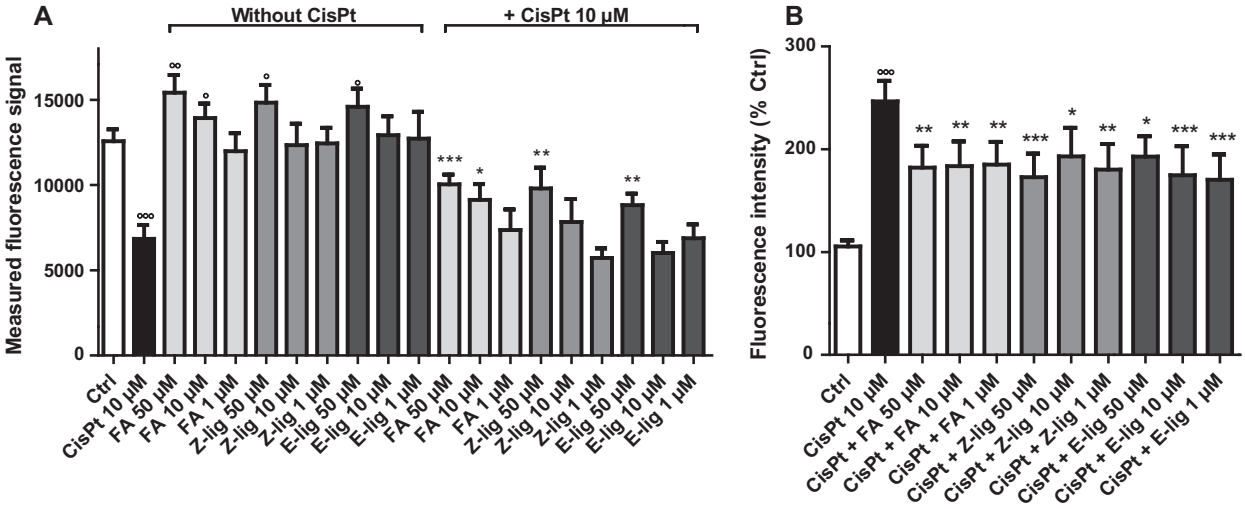

Fig. 8. QFIA of immunostained membranous β-catenin in HK-2 cells treated with test compounds for 48 h **(A)**. Fluorescence intensities (geometrical MFI) obtained for nuclear β-catenin of cells analyzed with a flow cytometry technique **(B)**. Results are displayed as means ± SD of 4 independent experiments (°: $p < 0.05$; °°: $p < 0.01$; °°°: $p < 0.001$ compared to control group/*: $p < 0.05$; **: $p < 0.01$; ***: $p < 0.001$ compared to CisPt group).

Table 1
Summary of the effects observed along the nephroprotective activity tests.

	Z-lig	E-lig	FA
Improvement in cell survival	0	–	++
Apoptosis reduction	++	0	+++
Antioxidant (radical scavenging)	0	0	+++
In cellulo oxidative stress restriction	+++	+++	0
Limitation of ECM synthesis	0	0	+++
Promotion of membranous β-catenin acquisition (without CisPt)	+	+	++
Maintain of membranous β-catenin (with CisPt)	+	+	++
Limitation of β-catenin relocalization	++	++	++
Proliferation enhancement	++	++	+++
Migration speed enhancement	0	–	+++

Presumably beneficial effects range from "+" to "+++", whereas the absence of effect is represented by a "0". The code "–" indicates a possible deleterious effect.

In the present study, 3 compounds isolated from *A. sinensis* have been assessed for their potential nephroprotective activity towards key phenomena involved in CisPt-induced AKI. The effects observed for each compound are summarized in Table 1.

4. Discussion

The major drawback of CisPt treatment resides in its nephrotoxicity. As this chemotherapeutic drug severely alters RPTECs integrity – resulting in an AKI for about 20–30% of patients – its dose has to be limited, what may compromise the cancer therapy (Yao et al., 2007). For now, the only strategy used in clinical practice to reduce the risk of AKI onset is to hydrate patients sufficiently and ensure adequate diuresis. New pharmacological approaches that could limit the nephrotoxicity of CisPt remain to be developed.

CisPt is filtered by the glomerulus, and notably penetrates RPTECs via the basolateral organic cation transporter (OCT2) (Yao et al., 2007) where it binds to cell's DNA (Jamieson and Lippard, 1999). Evidences suggest that cellular damage mediated by the generation of ROS play an important role in the pathogenesis of CisPt-induced AKI (Cummings and Schnellmann, 2002; Davis et al., 2001). The major consequence of these phenomena is the induction of cell death via apoptosis or necrosis; the latter has been show to occur at high doses of CisPt (Yao et al., 2007). A cell cycle arrest attributed to DNA damage (dos Santos et al., 2012), the production of ECM associated with fibrotic healing and phenotypic dedifferentiation processes (Zeisberg and Duffield, 2010) are also commonly observed.

Thus, preventing the onset of AKI could limit the development of interstitial fibrosis and the further progression to end-stage renal disease.

4.1. Prevention of cell death via apoptosis

In reducing cellular death along the tubules by lowering the apoptosis rate, the nephrons function and structure could be preserved.

The resazurin assay indicates that FA could efficiently limit the mortality of cells treated with CisPt after 24, 48 and 72 h in a dose dependent manner. This was confirmed by the determination of apoptosis rates: at the 3 time-points, apoptosis rates were enhanced between 3.0 and 4.0-fold over control after incubation with CisPt. FA lowered the proportion of apoptotic cells in a dose-dependent manner. The higher dose, 50 µM FA, could however fully reverse neither CisPt-associated death, nor apoptosis.

Surprisingly, Z-lig and E-lig, which were tested at 50 µM for their ability to reduce CisPt-induced apoptosis – despite their lack of activity on cellular viability – also exhibited a capacity to reduce the apoptosis rates (although this effect was of moderate intensity for E-lig). These results seem conflicting; but one could expect other processes to be involved in the parameters affecting the overall cellular viability in the presence of CisPt (e.g. proliferation arrest, autophagy (Kaushal et al., 2008), cell detachment, etc.). The lack of apparent positive effect on cell survival could be considered as a reason on its own for not fostering on Z-lig when screening for nephroprotective compounds. Indeed, according to the well-known structure–function relationship, any loss of viable RPTECs is directly correlated to a loss of renal function; and thus, favoring a high survival rate appears as a key phenomenon for the alleviation of CisPt-triggered AKI.

The use of higher concentrations in CisPt (e.g. IC_{50}), in an attempt to highlight a positive effect of Z-lig on cell survival, should be investigated in a new study.

Finally, the highest dose of E-lig was associated with a decreased viability as compared to CisPt alone. The resazurin test performed in the absence of CisPt also indicated a lower metabolic

activity. That is however not related to a higher cellular mortality; indeed, the quantification of proteins did not reveal any decrease when the cells were treated with 50 μM E-lig alone. This suggests that E-lig lowered the metabolic activity of cells (perhaps in lowering their respiratory rate) without affecting their survival. To our knowledge, it is the first time that such an effect is described for E-ligustilide; the relevance of this activity should be investigated in *in vivo* studies. This compound is rather widely consumed as part of medicinal and edible herbs (such as *A. sinensis*, *Ligusticum striatum*, lovage, celery and celeriac)and would not be expected to demonstrate toxic properties, at least at nutritional doses.

The reduction of metabolic activity induced by E-lig could not be observed after Z-lig treatment. Although literature reports numerous bioactivities for Z-lig, little is known about its E-isomer and metabolites. Indeed, ligustilides are acknowledged as rather unstable compounds capable of undergoing degradation and structural rearrangement; E-lig being more unstable than Z-lig (Yang et al., 2012). Further structure–activity studies are needed before formulating any hypothesis, particularly regarding the cellular target(s) of E-lig.

The decreases in metabolic activity observed for the combination of 10 μM CisPt and 50 μM E-lig did not display any additive or synergistic profile. On the contrary, the viability rates were somewhat higher than expected for this co-treatment; this being probably a consequence of the trends observed in apoptosis experiments.

In an attempt to protect the kidneys with FA, a theoretical risk would be that the protection extends to cancer cells as well, thus leading to chemotherapy failure. Previous reports actually indicate that FA could enhance CisPt, carboplatin and 5-fluorouracil cytotoxicities on HeLa and K562 cell lines; antiproliferative effects have also been observed on Hela cells (Mancuso and Santangelo, 2014). Such apparently selective protection effects are worthy to further investigate.

4.2. Effects on oxidative stress

Oxidative stress is a cornerstone of CisPt nephrotoxicity *in vivo* (Yao et al., 2007). It directly acts on key biomolecules such as DNA, proteins and lipids, and modifies their structures.

After incubation of HK-2 cells for 24 h with CisPt, the generation of ROS/RNS was increased to 1.5-fold over control. The addition of 50 μM Z- or E-ligustilides reversed the H_2DCF-DA oxidation to levels similar to those obtained for controls. FA however did not manage to alleviate CisPt-induced oxidative stress augmentation.

In preliminary experiments, each of the tested compounds was evaluated for its capacity to scavenge free radicals via the DPPH assay. If FA revealed a promising antioxidant capacity (TEAC = 2.1), both ligustilides exhibited a poor ability to scavenge DPPH (TEAC > 50) and were not expected to reduce the oxidative stress in HK-2 cells. However, the antioxidant properties of ligustilides have been previously reported, and related to induction of enzymes involved in the neutralization of ROS (*i.e.* superoxide dismutase, catalase and glutathione peroxidase) (Chao and Lin, 2011). It is quite noteworthy that such mechanisms are more effective in lowering the intracellular oxidative stress than the addition of a reducing agent.

This phenomenon does not appear to be sufficient to avoid cell death: if Z-lig reduced both oxidative stress and apoptosis, it did not allow enhancing cell survival following CisPt treatment. In parallel, E-lig, which also demonstrated an interesting antioxidant effect, did not reduce the number of cells undergoing apoptosis and death.

Previous studies have reported the activation of Nrf2 pathway by Z-ligustilide, and the subsequent transcription of genes coding for the expression of antioxidant enzymes such as NQO1 (NAD(P)H: quinone oxidoreductase), glutathion-S-transferase ou heme oxygenase (Peng et al., 2013; Saw et al., 2013).

4.3. Promotion of tubular regeneration

Defects in the regeneration of tubules can lead to a fibrotic repair (Wynn, 2010). Thus, enhancing the proliferation and migration capacities of healthy RPTECs is likely to alleviate the severity and duration of AKI.

To evaluate the proliferative potential of HK-2 cells, their Ki-67 index was assessed. This protein is present on the nuclei of proliferating cells (*i.e.* in G1, S, G2 and M phases of the cell cycle) and remains absent in quiescent cells (G0) (Urruticoechea et al., 2005). It is therefore used in clinical practice to evaluate the proliferative potential of cancer cells, but it has also been used *in vitro* and *in vivo* for the assessment of RPTECs regeneration (Bunel et al., 2014b; Docherty et al., 2006; Pozdzik et al., 2008).

Upon treatment with CisPt, the proportion of Ki-67 positive cells rose of 2.2-fold, what might be interpreted as corresponding to higher proliferation rates. However, the flow cytometry analysis of the cell cycle phases distribution invalidates this observation: the CisPt treatment massively increased the proportion of G2/M cells (9.4-fold) as compared to the control condition, leading to falsely proliferation-positive cells. This confirms previous observations that CisPt triggers a cell cycle arrest at the G2/M checkpoint (Jamieson and Lippard, 1999).

Proliferation was induced by FBS treatment, as observed via the Ki-67 index (rise of 3.3-fold as compared to Ctrl) and cell cycle phases distribution (2.1-fold increase in the proportion of G2/M cells, associated with a 0.9-fold decrease in G0/G1 cells, as compared to Ctrl).

The 3 studied ASAC were capable of increasing the Ki-67 index in a dose-dependent manner; FA showed the highest efficacy over the 3 tested concentrations (2.3, 2.3 and 1.9-fold increases for concentrations of 50, 10 and 1 μM, respectively). Z- and E-lig also increased Ki-67 indices, ranging from 2.0 and 1.1-fold over control whatever the dose. The cell cycle analysis yielded patterns that were similar to those obtained for FBS treatment, suggesting that the elevation in Ki-67 index can be attributed to a real effect on proliferation, rather than a cell cycle arrest as observed for CisPt treatment.

These data suggest that ASAC promotes the proliferation of healthy HK-2 cells, probably in stimulating G1 phase entering, and thus lowering the proportion of G0 cells. Evidences for this activity were brought for FA, which enhanced the metabolic activity of cells treated for 48 or 72 h, as observed with the resazurin assay (Fig. 2S), and produced higher amounts of proteins after 72 h (Fig. 3S).

A wound healing assay examined the cellular migration, highlighting the capacity of FA to enhance the motility of HK-2 cells in a dose-dependent manner: the migration speed was found to be enhanced by 1.7, 1.6 and 1.4-fold as compared to control conditions for concentrations of 50, 10 and 1 μM FA, respectively. This result is consistent with previous data reporting an enhanced migration ability of fibroblasts upon FA treatment (Hsiao et al., 2012). Z-lig did not produce any modification. The highest dose of E-lig could even lower the migration rates as compared to the control condition, perhaps as a consequence of a lower metabolic activity; taken together, these results suggest a possible anticancer activity of E-lig requiring further investigations.

Altogether, these effects support that FA could be used to promote tubular regeneration following AKI, a condition during which the loss of RPTECs is associated with a transient – but not fully irreversible – loss of tubular structure and function (Bucaloiu et al., 2012).

4.4. Limitation of collagen deposition

Collagen is an ECM component produced by cells during abnormal wound healing process and which acts as a pro-fibrotic factor (Wynn, 2007). In preventing its deposition in damaged tubules, the integrity of the interstitial compartment may be preserved.

PSR staining is a convenient assay although not entirely specific for collagen; the method allows distinguishing between types I and III collagens under polarized light, but also stains collagen IV in basal membrane, as well as other reticular fibers present in the ECM (Junqueira et al., 1979; Puchtler et al., 1973). Although other methods (including hydroxyproline quantification, collagen immunohistochemistry or immunofluorescence staining) could lead to a more accurate assessment of collagen(s), PSR staining clearly indicates collagen/ECM deposition (Pape et al., 2003).

Among the 3 tested compounds, only FA could reduce the amount of CisPt-induced collagen deposition in a dose-dependent manner: it dropped to 112 ± 2, 120 ± 3 and 126 ± 3% for doses of 50, 10 and 1 μM FA, as compared to 135 ± 4% for CisPt treatment alone. It could therefore be useful to avoid the replacement of functional tissues by ECM, and could probably attenuate fibrotic repairs associated with AKI.

4.5. Localization of β-catenin

β-catenin plays a dual role in RPTECs: *(i)* in linking E-cadherin to α-catenin (which in turn binds the actin microfilaments of the cytoskeleton), it is involved in cell adhesion; and *(ii)* in case of cellular injury, intercellular junction can disrupt, and β-catenin relocalizes into the nucleus after reconfiguration into a distinct form (Gottardi and Gumbiner, 2004). If membranous β-catenin participates to the integrity of the epithelial phenotype (Zeisberg and Neilson, 2009), its relocalizing form binds to Tcf/Lef factors and rules the transcription of genes involved in fibrosis (Bozic et al., 2011). This property has been used to assess the dedifferentiation processes in altered RPTECs.

4.6. Membranous β-catenin

In a QFIA of HK-2 cells treated for 48 h with CisPt, we highlighted a massive loss of fluorescence attributed to membranous β-catenin as compared to the control conditions. However, co-treatment with 50 and 10 μM FA and 50 μM of both ligustilides restrained this loss, indicating that they were able to prevent HK-2 cells from losing their epithelial phenotype. The most intense effect was observed for 50 μM FA treatment, which restrained membranous β-catenin loss to 1.2-fold vs. control as compared to the 1.8-fold decrease observed after CisPt treatment. In maintaining cell–cell interactions, this may also prevent cells from detaching and enhance overall survival.

Furthermore, cells treated with 50 μM ASAC and 10 μM FA in the absence of CisPt displayed higher amounts of membranous β-catenin as compared to control; the highest increase (1.2-fold) was observed for 50 μM FA. This data suggests that both compounds could play a beneficial role in tubular regeneration by helping RPTECs acquiring their epithelial phenotype.

4.7. Internal β-catenin

Reported evidences suggest that inhibition of the intracellular β-catenin pathway impedes the progression of renal fibrosis (Hao et al., 2011; He et al., 2011).

CisPt increased the proportion of relocalizing β-catenin of about 2.5-fold over the control. All of the tested ASAC limited this increase in a magnitude that was not related to their concentration (1.7-fold over control in average). FA, Z-lig and E-lig may thus be effective in reducing the transcription of genes involved in fibrotic processes.

5. Conclusion

The data presented in this work support the possibility of using FA, Z-lig and E-lig as nephroprotective drugs. Indeed, the 3 tested compounds present various positive effects towards phenomena implied in CisPt-triggered AKI and kidney fibrosis. Despite its inability to reduce oxidative stress, FA however stands as the most promising nephroprotective drug lead *in vitro*: *(i)* it can reduce CisPt-induced apoptosis and enhance overall cell viability; *(ii)* it improves regeneration capacities of RPTECs by stimulating both cellular proliferation and motility; *(iii)* it limits the amount of collagen synthesized upon CisPt treatment which would reduce the production of ECM; and *(iv)* it can help in the acquisition of membranous β-catenin (further supporting a beneficial activity in regeneration processes) and can partly avoid its nuclear relocalization, suggesting that the β-catenin pathway involved in kidney fibrosis might be impeded.

Ferulic acid appears as a promising drug lead deserving further preclinical investigation. Z- and E-ligustilides may also possess some renoprotective effects, notably conferred by their ability to prevent the rise in oxidative stress induced by CisPt treatment. Further studies should investigate a possible synergistic effect for the combination of ferulic acid and Z-ligustilide which are both considered *A. sinensis* major bioactive compounds.

Funding

Valérian Bunel is a fellow of the Fonds de la Recherche Scientifique – FNRS (FRIA grant).

Conflict of Interest

The authors declare that there are no conflicts of interest.

Transparency Document

The Transparency document associated with this article can be found in the online version.

Acknowledgements

We are grateful to Complemedis AG (Trimbach, Switzerland) for kindly providing bulk Radix Angelicae sinensis. Thanks are also expressed to C. Husson, E. De Prez, M. Faes and O. Vaillant for technical assistance.

Appendix A. Supplementary material

Supplementary data associated with this article can be found, in the online version, at http://dx.doi.org/10.1016/j.tiv.2014.12.017.

References

Anonymous, 2011. FlowJo, data analysis software for flow cytometry, In: Inc., T.S. (Ed.), FlowJo Advanced Tutorial, 7.6.2 ed., Tree Star Inc., Ashland, p. 37.

Barabas, K., Milner, R., Lurie, D., Adin, C., 2008. Cisplatin: a review of toxicities and therapeutic applications. Vet. Comp. Oncol. 6, 1–18.

Bozic, M., de Rooij, J., Parisi, E., Ortega, M.R., Fernandez, E., Valdivielso, J.M., 2011. Glutamatergic signaling maintains the epithelial phenotype of proximal tubular cells. J. Am. Soc. Nephrol. 22, 1099–1111.

Bucaloiu, I.D., Kirchner, H.L., Norfolk, E.R., Hartle, J.E., Perkins, R.M., 2012. Increased risk of death and *de novo* chronic kidney disease following reversible acute kidney injury. Kidney Int. 81, 477–485.

Bunel, V., Antoine, M.H., Nortier, J., Duez, P., Stevigny, C., 2014a. Potential nephroprotective effects of the Chinese herb *Angelica sinensis* against cisplatin tubulotoxicity. Pharm. Biol. http://dx.doi.org/10.3109/13880209.2014.951726. [Epub ahead of print].

Bunel, V., Antoine, M.H., Nortier, J., Duez, P., Stevigny, C., 2014b. Protective effects of schizandrin and schizandrin B towards cisplatin nephrotoxicity *in vitro*. J. Appl. Toxicol. 34, 1311–1319.

Cai, Q., Li, X., Wang, H., 2001. Astragali and Angelica protect the kidney against ischemia and reperfusion injury and accelerate recovery. Chin. Med. J. (Engl.) 114, 119–123.

Chao, W.W., Lin, B.F., 2011. Bioactivities of major constituents isolated from *Angelica sinensis* (Danggui). Chin. Med. 6, 1–7.

Chen, X.P., Li, W., Xiao, X.F., Zhang, L.L., Liu, C.X., 2013. Phytochemical and pharmacological studies on Radix *Angelicae sinensis*. Chin. J. Nat. Med. 11, 577–587.

Cummings, B.S., Schnellmann, R.G., 2002. Cisplatin-induced renal cell apoptosis: caspase 3-dependent and -independent pathways. J. Pharmacol. Exp. Ther. 302, 8–17.

Davis, C.A., Nick, H.S., Agarwal, A., 2001. Manganese superoxide dismutase attenuates Cisplatin-induced renal injury: importance of superoxide. J. Am. Soc. Nephrol. 12, 2683–2690.

Docherty, N.G., O'Sullivan, O.E., Healy, D.A., Murphy, M., O'Neill, A.J., Fitzpatrick, J.M., Watson, R.W., 2006. TGF-beta1-induced EMT can occur independently of its proapoptotic effects and is aided by EGF receptor activation. Am. J. Physiol. Renal. Physiol. 290, F1202–F1212.

dos Santos, N.A., Carvalho Rodrigues, M.A., Martins, N.M., dos Santos, A.C., 2012. Cisplatin-induced nephrotoxicity and targets of nephroprotection: an update. Arch. Toxicol. 86, 1233–1250.

Geback, T., Schulz, M.M., Koumoutsakos, P., Detmar, M., 2009. TScratch: a novel and simple software tool for automated analysis of monolayer wound healing assays. Biotechniques 46, 265–274.

Gottardi, C.J., Gumbiner, B.M., 2004. Distinct molecular forms of beta-catenin are targeted to adhesive or transcriptional complexes. J. Cell Biol. 167, 339–349.

Hao, S., He, W., Li, Y., Ding, H., Hou, Y., Nie, J., Hou, F.F., Kahn, M., Liu, Y., 2011. Targeted inhibition of b-catenin/CBP signaling ameliorates renal interstitial fibrosis. J. Am. Soc. Nephrol. 22, 1642–1653.

Havasi, A., Borkan, S.C., 2011. Apoptosis and acute kidney injury. Kidney Int. 80, 29–40.

He, W., Kang, Y.S., Dai, C., Liu, Y., 2011. Blockade of Wnt/beta-catenin signaling by paricalcitol ameliorates proteinuria and kidney injury. J. Am. Soc. Nephrol. 22, 90–103.

Hilal, G., Albert, C., Vallée, M., 2005. Mécanismes impliqués dans la néphrotoxicité. Ann. Biol. Clin. Qué. 42, 29–35.

Hsiao, C.Y., Hung, C.Y., Tsai, T.H., Chak, K.F., 2012. A study of the wound healing mechanism of a traditional Chinese Medicine, *Angelica sinensis*, using a proteomic approach. Evid. Based Complement Alternat. Med. 2012, 1–14.

Hu, Q., Noor, M., Wong, Y.F., Hylands, P.J., Simmonds, M.S., Xu, Q., Jiang, D., Hendry, B.M., 2009. *In vitro* anti-fibrotic activities of herbal compounds and herbs. Nephrol. Dial. Transplant. 24, 3033–3041.

Jamieson, E.R., Lippard, S.J., 1999. Structure, recognition, and processing of cisplatin-DNA adducts. Chem. Rev. 99, 2467–2498.

Junqueira, L.C., Bignolas, G., Brentani, R.R., 1979. Picrosirius staining plus polarization microscopy, a specific method for collagen detection in tissue sections. Histochem. J. 11, 447–455.

Kaushal, G.P., Kaushal, V., Herzog, C., Yang, C., 2008. Autophagy delays apoptosis in renal tubular epithelial cells in cisplatin cytotoxicity. Autophagy 4, 710–712.

Lee, S.B., Kalluri, R., 2010. Mechanistic connection between inflammation and fibrosis. Kidney Int. 78, S22–S26.

Li, X., Wang, H., 2005. Chinese herbal medicine in the treatment of chronic kidney disease. Adv. Chronic Kidney Dis. 12, 276–281.

Liu, Y., 2010. New insights into epithelial-mesenchymal transition in kidney fibrosis. J. Am. Soc. Nephrol. 21, 212–222.

Low Dog, T., 2005. Menopause: a review of botanical dietary supplements. Am. J. Med. 118 (Suppl 12B), 98–108.

Mancuso, C., Santangelo, R., 2014. Ferulic acid: pharmacological and toxicological aspects. Food Chem. Toxicol. 65, 185–195.

Megyesi, J., Andrade, L., Vieira Jr., J.M., Safirstein, R.L., Price, P.M., 2002. Coordination of the cell cycle is an important determinant of the syndrome of acute renal failure. Am. J. Physiol. Renal. Physiol. 283, F810–F816.

Meng, L.Q., Tang, J.W., Wang, Y., Zhao, J.R., Shang, M.Y., Zhang, M., Liu, S.Y., Qu, L., Cai, S.Q., Li, X.M., 2011. Astragaloside IV synergizes with ferulic acid to inhibit renal tubulointerstitial fibrosis in rats with obstructive nephropathy. Br. J. Pharmacol. 162, 1805–1818.

Nortier, J., Sculier, J.P., 2011. Thoracic malignancies, cisplatin and renal function. Eur. Respir. J. 37, 760–761.

Pabla, N., Dong, Z., 2008. Cisplatin nephrotoxicity: mechanisms and renoprotective strategies. Kidney Int. 73, 994–1007.

Pape, L., Henne, T., Offner, G., Strehlau, J., Ehrich, J.H., Mengel, M., Grimm, P.C., 2003. Computer-assisted quantification of fibrosis in chronic allograft nephropaty by picosirius red-staining: a new tool for predicting long-term graft function. Transplantation 76, 955–958.

Peng, B., Zhao, P., Lu, Y.P., Chen, M.M., Sun, H., Wu, X.M., Zhu, L., 2013. Z-ligustilide activates the Nrf2/HO-1 pathway and protects against cerebral ischemia-reperfusion injury *in vivo* and *in vitro*. Brain Res. 1520, 168–177.

Pozdzik, A.A., Salmon, I.J., Debelle, F.D., Decaestecker, C., Van den Branden, C., Verbeelen, D., Deschodt-Lanckman, M.M., Vanherweghem, J.L., Nortier, J.L., 2008. Aristolochic acid induces proximal tubule apoptosis and epithelial to mesenchymal transformation. Kidney Int. 73, 595–607.

Puchtler, H., Waldrop, F.S., Valentine, L.S., 1973. Polarization microscopic studies of connective tissue stained with picro-sirius red FBA. Beiträge zur Pathol. 150, 174–187.

Ryan, M.J., Johnson, G., Kirk, J., Fuerstenberg, S.M., Zager, R.A., Torok-Storb, B., 1994. HK-2: an immortalized proximal tubule epithelial cell line from normal adult human kidney. Kidney Int. 45, 48–57.

Saw, C.L., Wu, Q., Su, Z.Y., Wang, H., Yang, Y., Xu, X., Huang, Y., Khor, T.O., Kong, A.N., 2013. Effects of natural phytochemicals in *Angelica sinensis* (Danggui) on Nrf2-mediated gene expression of phase II drug metabolizing enzymes and anti-inflammation. Biopharm. Drug Dispos. 34, 303–311.

Song, J., Meng, L., Li, S., Qu, L., Li, X., 2009. A combination of Chinese herbs, *Astragalus membranaceus var. mongholicus* and *Angelica sinensis*, improved renal microvascular insufficiency in 5/6 nephrectomized rats. Vascul. Pharmacol. 50, 185–193.

Urruticoechea, A., Smith, I.E., Dowsett, M., 2005. Proliferation marker Ki-67 in early breast cancer. J. Clin. Oncol. 23, 7212–7220.

Valcu, M., Valcu, C.M., 2011. Data transformation practices in biomedical sciences. Nat. Methods 8, 104–105.

Wang, H., Li, J., Yu, L., Zhao, Y., Ding, W., 2004. Antifibrotic effect of the Chinese herbs, *Astragalus mongholicus* and *Angelica sinensis*, in a rat model of chronic puromycin amino nucleoside nephrosis. Life Sci. 74, 1645–1658.

Wojcikowski, K., Wohlmuth, H., Johnson, D.W., Rolfe, M., Gobe, G., 2009. An *in vitro* investigation of herbs traditionally used for kidney and urinary system disorders: potential therapeutic and toxic effects. Nephrology 14, 70–79.

Wynn, T.A., 2007. Common and unique mechanisms regulate fibrosis in various fibroproliferative diseases. J. Clin. Invest. 117, 524–529.

Wynn, T.A., 2010. Fibrosis under arrest. Nat. Med. 16, 523–525.

Xu, Q., Norman, J.T., Shrivastav, S., Lucio-Cazana, J., Kopp, J.B., 2007. *In vitro* models of TGF-beta-induced fibrosis suitable for high-throughput screening of antifibrotic agents. Am. J. Physiol. Renal Physiol. 293, F631–F640.

Yang, J.-Y., Chen, H.-H., Wu, J., Gong, S.-X., Chen, C.-Q., Zhang, T.-J., Wang, M.-J., 2012. Advances in studies on pharmacological functions of ligustilide and their mechanisms. Chinese Herbal Med. 4, 26–32.

Yang, L., Besschetnova, T.Y., Brooks, C.R., Shah, J.V., Bonventre, J.V., 2010. Epithelial cell cycle arrest in G2/M mediates kidney fibrosis after injury. Nat. Med. 16, 535–543 (531p following 143).

Yao, X., Panichpisal, K., Kurtzman, N., Nugent, K., 2007. Cisplatin nephrotoxicity: a review. Am. J. Med. Sci. 334, 115–124.

Zeisberg, M., Duffield, J.S., 2010. Resolved: EMT produces fibroblasts in the kidney. J. Am. Soc. Nephrol. 21, 1247–1253.

Zeisberg, M., Neilson, E.G., 2009. Biomarkers for epithelial-mesenchymal transitions. J. Clin. Invest. 119, 1429–1437.